Cell Research (2007) 17:1030-11040.

www.nature.com/cr

ORIGINAL ARTICLE

Involvement of sphingoid bases in mediating reactive oxygen intermediate production and programmed cell death in *Arabidopsis*

Lihua Shi[1, 2, *], Jacek Bielawski[3, *], Jinye Mu[1, 2, *], Haili Dong[1, 2], Chong Teng[1, 2], Jian Zhang[1], Xiaohui Yang[1], Nario Tomishige[4], Kentaro Hanada[4], Yusuf A Hannun[3], Jianru Zuo[1]

[1]National Key Laboratory of Plant Genomics, Institute of Genetics and Developmental Biology, Chinese Academy of Sciences, Datun Road, Beijing 100101, China; [2]Graduate School, Chinese Academy of Sciences, 19A Yuquan Road, Beijing 100049, China; [3]Department of Biochemistry and Molecular Biology, Medical University of South Carolina, 173 Ashley Avenue, Charleston, SC 29425, USA; [4]Department of Biochemistry and Cell Biology, National Institute of Infectious Diseases, 1-23-1, Toyama, Shinjuku-ku, Tokyo 162-8640, Japan

Sphingolipids have been suggested to act as second messengers for an array of cellular signaling activities in plant cells, including stress responses and programmed cell death (PCD). However, the mechanisms underpinning these processes are not well understood. Here, we report that an *Arabidopsis* mutant, *fumonisin B1 resistant11-1* (*fbr11-1*), which fails to generate reactive oxygen intermediates (ROIs), is incapable of initiating PCD when the mutant is challenged by fumonisin B_1 (FB_1), a specific inhibitor of ceramide synthase. Molecular analysis indicated that *FBR11* encodes a long-chain base1 (LCB1) subunit of serine palmitoyltransferase (SPT), which catalyzes the first rate-limiting step of *de novo* sphingolipid synthesis. Mass spectrometric analysis of the sphingolipid concentrations revealed that whereas the *fbr11-1* mutation did not affect basal levels of sphingoid bases, the mutant showed attenuated formation of sphingoid bases in response to FB_1. By a direct feeding experiment, we show that the free sphingoid bases dihydrosphingosine, phytosphingosine and sphingosine efficiently induce ROI generation followed by cell death. Conversely, ROI generation and cell death induced by dihydrosphingosine were specifically blocked by its phosphorylated form dihydrosphingosine-1-phosphate in a dose-dependent manner, suggesting that the maintenance of homeostasis between a free sphingoid base and its phosphorylated derivative is critical to determining the cell fate. Because alterations of the sphingolipid level occur prior to the ROI production, we propose that the free sphingoid bases are involved in the control of PCD in *Arabidopsis*, presumably through the regulation of the ROI level upon receiving different developmental or environmental cues.

Keywords: *Arabidopsis, fumonisin B1 resistant11-1,* PCD, ROIs, sphingolipids

Cell Research (2007) **17**:1030-1040. doi: 10.1038/cr.2007.100; published online 4 December 2007

Introduction

In eukaryotic organisms, programmed cell death (PCD) is an important mechanism to control normal growth and development as well as defense responses to a variety of biotic and abiotic stresses. In plants, PCD is essential for a number of developmental processes. The best-known examples include the specification of unisexual floral organs, the formation of the tracheary elements and senescence [1, 2]. Moreover, an impressive body of evidence obtained from studies on plant-pathogen interactions, particularly those derived from genetic studies on *Arabidopsis*, has provided substantial insight into the PCD mechanism in

*These authors contributed equally to this work.
Correspondence: Jianru Zuo
Fax: +086-010-6487 3428
E-mail: jrzuo@genetics.ac.cn
Received 29 October 2007; revised 10 November 2007; accepted 12 November 2007; published online 4 December 2007

plant cells [3-7]. One of the most commonly observed PCD forms triggered by pathogen infection is the so-called hypersensitive response (HR), which involves the formation of reactive oxygen intermediates (ROIs) and nitric oxide, and largely relies on the salicylic acid signaling pathway [3, 8, 9]. However, little is known about the biochemical mechanism of PCD in plant cells.

Sphingolipids are a diverse group of lipids that contain a relatively large hydrophobic moiety, known as ceramides that include a sphingoid or long-chain base (LCB) amide-linked to a fatty acid. Sphingolipids are not only essential components of cellular membranes, but also act as second messengers to regulate stress responses, cell proliferation and apoptosis [10-13]. *De novo* biosynthesis of sphingolipids is initiated by the condensation of serine and palmitoyl-CoA to produce 3-ketosphinganine (3-KDS) [10, 13]. This reaction is catalyzed by serine palmitoyltransferase (SPT; EC 2.3.1.50), a heterodimeric complex consisting of two subunits of LCB1 and LCB2 localized in the endoplasmic reticulum (ER) [14]. 3-KDS is first reduced to sphinganine or dihydrosphingosine (dh-sph) by 3-KDS reductase, and dh-sph is then converted into ceramides by (dihydro) ceramide synthase.

In higher plants, several studies suggested that fumonisin B_1 (FB_1) and *Alternaria alternate lycopersici* (AAL) toxin, two natural compounds that specifically inhibit ceramide synthase activity, cause apoptotic cell death in various species [15-20]. In *Arabidopsis*, FB_1-induced PCD depends on multiple signaling pathways, including those of jasmonate, ethylene, and salicylic acid [19]. More direct evidence was obtained from genetic studies. *Arabidopsis ACD11* encodes a sphingosine (sph) transfer protein, and a mutation in this gene causes a lesion mimic phenotype characteristic of apoptosis [21]. Similarly, mutations in *ACD5* cause a spontaneous cell death phenotype [22]. The *ACD5* wild type (WT) allele encodes a ceramide kinase, and a recombinant ACD5 protein has high specificity for ceramides but not other sphingolipids [23]. These observations suggest that the maintenance of sphingolipid homeostasis is important for properly regulating apoptosis in plant cells. The mechanism of sphingolipid-regulated PCD in plant cells, however, remains unclear.

In addition to a regulatory role in PCD, sphingolipids are also suggested to modulate stress responses. Recent studies revealed that sphingosine-1-phosphate (S1P) is involved in the regulation of the abscisic acid (ABA) pathway [24, 25], and S1P action appears to be mediated by physical interactions of a heterotrimeric G protein and a putative G protein-coupled receptor [25, 26]. Although a direct link between the ABA pathway and PCD has not been shown, the fact that many of the phytohormone-regulated physiological activities such as seed development and stress responses may directly or indirectly involve PCD implies a possible interplay between the two pathways, in which S1P or other sphingolipids may act as critical mediators.

Here, we report the identification and characterization of the *Arabidopsis fumonisin B_1 resistant11-1* (*fbr11-1*) mutant, which displayed a reduced sensitivity to the apoptosis-inducing agent FB_1. Molecular analysis indicated that *FBR11* encodes an LCB1 of SPT. The FB_1-induced PCD phenotype is correlated with massively increased concentrations of several sphingoid bases. A pharmacological approach showed that whereas dh-sph is a potent PCD inducer, its phosphorylated form dihydrosphingosine-1-phosphate (dh-S1P) acts specifically as an anti-apoptotic molecule. Moreover, the antagonistic effects of these compounds appear to be executed through the regulation of the ROI level, thereby controlling an apoptotic cell death program in plant cells.

Materials and Methods

Plant materials, growth conditions and genetic screen for fbr mutants

The Col-0 ecotype of *Arabidopsis thaliana* was used in this study. Unless otherwise indicated, plants were grown under a 16 h light/8 h dark cycle at 22 ºC in soil or on an MS medium [27] containing 3% sucrose and 0.8% agar.

A binary vector pER16 [28] was used for the generation of T-DNA lines by standard methods [29, 30]. Approximate 12 000 independent lines were screened for *fbr* mutants as described [20, 31]. Briefly, pooled T2 seeds (20 lines/pool; approximate 10 seeds/line) were germinated and grown on MS medium containing 1 μM FB_1 for 1-2 weeks. Putative *fbr* mutants were identified by visual inspection and then transferred onto a fresh MS medium without FB_1.

Chemicals and treatment

FB_1, paraquat and sphingoid bases (except phyto-S1P) were purchased from Sigma Inc., China and Hong Kong. Phyto-S1P was purchased from Avanti Polar Lipids (Alabaster, AL, USA). The following solvents were used for the preparation of stock solutions: water (paraquat), methanol (S1P), methanol/tetrahydrofuran/water (60/30/10%; v/v; phyto-S1P and dh-S1P) and dimethyl sulfoxide (DMSO; all others). Chemical treatment was carried out by directly germinating seeds on MS medium supplemented with appropriate chemicals or by spraying (2 ml per 90-mm Petri dish) plants germinated and grown on MS medium. The same concentrations of solvents were used as controls in all experiments. All experiments were repeated at least 5 times with commercial reagents and 2-3 times with homemade chemicals, and similar results were obtained. All data presented are representative results obtained by the use of commercial reagents.

Detection of cell death, superoxide, hydrogen peroxide and callose

Detection of superoxide, hydrogen peroxide and callose was performed by staining leaves with nitroblue tetrazolium (NBT), 3,3-diaminobenzidine (DAB) and aniline, respectively [32-34]. Cell death was examined by Evans Blue staining as described [33] with

minor modifications. Briefly, leaves samples were vacuum-infiltrated in 0.1% Evans Blue (w/v; Sigma) for 15 min and then maintained for 8 h under vacuum. After the staining, leaves were washed for three times (15 min each wash) with a phosphate-buffered saline containing 0.05% (v/v) Tween 20. All experiments were repeated at least 5 times, and at least 10 leaves collected from multiple seedlings (4-5-week-old) were inspected in each experiment. Penetration of the phenotype was usually higher than 80% (protoplast assay) and 90% (leaf assay) in these experiments, respectively.

Detection of nuclear DNA fragmentation in protoplasts was performed as previously described [31].

Analysis of sphingolipids

Measurement of sphingolipids was performed by Electrospray Ionization/Mass spectrum/Mass spectrum analysis on a Thermo Finnigan TSQ 7000 triple quadrupole mass spectrometer, operating in a Multiple Reaction Monitoring positive ionization mode as described [35]. Briefly, samples collected and frozen in liquid nitrogen were dried by lyophilizing at –50 ºC, and then ground into fine powder, which was then fortified with the internal standards (IS; C_{17} base D-erythro-sphingosine, C_{17} sphingosine-1-phosphate, N-palmitoyl-D-erythro-C_{13} sphingosine, heptadecanoyl-D-erythro-sphingosine and C6-Phyto-ceramide). Fifteen milligrams of dried powder were extracted with the ethyl acetate/iso-propanol/water (60/30/10%; v/v) solvent system. After evaporation and reconstitution in 100 µl of methanol, the samples were injected on the Surveyor/TSQ 7000 LC/MS system and gradient-eluted from the BDS Hypersil C8, 150 × 3.2 mm, 3 µm particle size column, with 1.0 mM methanolic ammonium formate/2 mM aqueous ammonium formate mobile phase system. Peaks corresponding to the target analytes and internal standards were collected and processed using the Xcalibur software system. Quantitative analysis was based on the calibration curves generated by spiking an artificial matrix with the known amounts of the target analyte synthetic standards and an equal amount of internal standards. The target analyte/IS peak areas ratios were plotted against analyte concentration, which were normalized to their respective ISs and compared to the calibration curves, using a linear regression model.

Molecular manipulations

All molecular manipulations were carried out according to standard methods [36]. The T-DNA tagged genomic sequence in the *fbr11-1* genome was identified by Thermal Asymmetric Interlaced-PCR (TAIL-PCR) as previously described [37, 38]. An *FBR11* genomic clone was obtained by PCR using PWO DNA polymerase (Roche Diagnostics Hong Kong, Hong Kong). Primers used in PCR were LCBCOMF (5′ GGT CGA CGG GAG ATA GGA GGA AGA AGA CTG ATT GA 3′) and LCBCOMB (5′ CCC TAG GGG ATT CTC AAC TCC ATT AAC GTC GAG GT 3′). The *FBR11* (At4g36480) genomic clone included a 1.5-Kb promoter sequence, starting from the 5′UTR of At4g36470 (in a head-to-head configuration with *FBR11*), to ensure inclusion of the entire promoter sequence. The PCR product, digested with *Sal*I and *Avr*II, was cloned into the *Xho*I and *Spe*I sites of pER8 [39]. The resulting construct was transformed into *A. tumefaciens* strain GV3101, which was used for transformation of *Arabidopsis* by vacuum infiltration [29]. DNA Southern and RNA Northern blotting analyses were carried out as described previously [38].

Analysis of gene expression by real time-PCR was performed essentially as previously described [40]. Primers used in the experiments described in Figure 3A and 3B were (all sequences are from 5′- to 3′-end):

P1: GCA GAG TCA GTA GCT TGA AGA TGT
P2: CGG CAA CAA CAC TAA GCT ACT TGA
P3: ACC AGA GAC TTA GCA GTT CAG GA
P4: CAA TAG GTG ATT CCC GGT TGC TTG

Results

Identification and genetic analysis of the fbr11-1 mutant

The *fbr11-1* mutant was identified in a genetic screen for fumonisin B_1-resistant mutants as described [20, 31]. Whereas the growth and development of WT plants were severely inhibited by FB_1, the *fbr11-1* mutant plant displayed substantial resistance to the toxin (Figure 1A). However, in the absence of FB_1, the *fbr11-1* mutant plant did not have detectable morphological alterations under different light or temperature conditions (Figure 1B and data not shown).

In a cross between *fbr11-1* and WT plants, all tested F1 progeny (33) were sensitive to FB_1, indicating that the mutation was recessive. In F2 progeny obtained from self-pollinated F1 plants, the mutation segregated in a 1:3 ratio (FB_1 resistant:sensitive =123:450, χ^2=3.423; p<0.05), suggesting that the mutant phenotype was caused by a mutation in a single nuclear gene.

The programmed cell death phenotype of fbr11-1

Compared with massive cell death induced by FB_1 in WT plants, essentially no cell death was detected in *fbr11-1* (Figure 1C) as revealed by Evans Blue staining. This suggests that the mutant phenotype was likely caused by the failure of a toxin-evoked cell death program. Moreover, the FB_1-induced cell death was accompanied by substantial deposition of callose in leaves of WT plants, which was not observed in leaves of *fbr11-1* plants (Figure 1D). To further investigate the molecular basis of the *fbr11-1* phenotype, we examined the accumulation of ROIs in both WT and *fbr11-1* leaves under different conditions. As shown in Figure 1E, the generation of superoxide (stained by NBT) was strongly induced by FB_1 in WT plants. By contrast, no superoxide accumulation was detected in *fbr11-1* under identical assay conditions. Similar results were obtained when stained with DAB (staining for hydrogen peroxide) (Figure 1F). Most experiments described hereafter were carried out by both NBT and DAB staining, and similar results were obtained. For concise reasons, we only show NBT staining data, and collectively refer to these two species as ROIs. Data presented in this section suggest that the absence of cell death in the mutant was likely caused by the lack of ROI production.

Nuclear DNA fragmentation is a hallmark of apoptotic

cells. To reveal whether nuclear DNA fragmentation occurred in FB_1-treated cells, we employed the TUNEL method to examine WT and *fbr11-1* protoplasts treated with or without the toxin (Figure 2). In untreated protoplasts derived from both WT and *fbr11-1* leaves, each cell contained a single condensed nucleus as revealed by staining with Hoechst 33342, a non-specific DNA dye, and no DNA fragmentation was detected in these protoplasts. Upon treatment with FB_1, significant DNA fragmentation was detected by TUNEL staining of WT protoplasts. By contrast, under the same conditions, *fbr11-1* protoplasts showed a phenotype indistinguishable from that of untreated controls (Figure 2). The TUNEL positive signals were routinely detected in WT protoplasts within 8-10 h after exposure to FB_1, whereas cell death was only detectable after a longer treatment of 22-24 h. On the other hand, in the leaflet assay, ROI generation could be detected 3-6 h after the FB_1 treatment but was barely detectable within 3 h of the treatment. Cell death induced by the compound was again detected 22-24 h after the treatment. The above results suggested that both ROI generation and DNA fragmentation occurred prior to cell death, which are characteristics of a controlled apoptotic program rather than a necrotic cell death effect. Based on the data presented above, we concluded that the *fbr11-1* mutant was incapable of initiating PCD induced by FB_1, presumably resulting from the failure to generate ROIs under these conditions.

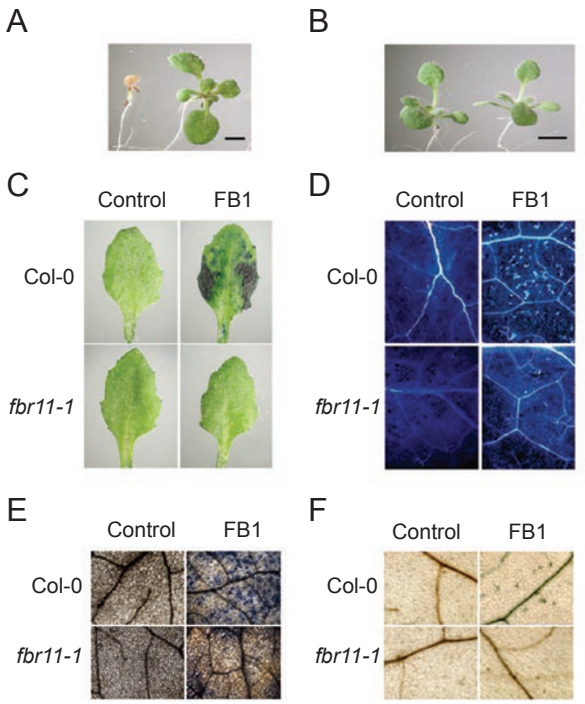

Figure 1 The *fbr11-1* mutant phenotype. **(A)** Two-week-old WT (left) and *fbr11-1* seedlings germinated and grown on MS medium containing 1 μM FB_1. **(B)** Two-week-old of the same plants germinated and grown on MS medium. **(C)** Cell death induced by FB_1. Three-week-old WT and *fbr11-1* plants were treated with methanol (0.1%; control) or 2 μM FB_1 for 24 h by spraying. Leaves were then detached from treated plants and stained with Evans Blue. Dead cells were stained blue. **(D)** The deposition of callose induced by FB_1. Plants were treated as described in **(C)** for 24 h, and leaves were harvested and stained with aniline. Callose deposition was visible as blue fluorescence. **(E)** The accumulation of superoxide induced by FB_1. Plants were treated as described in **(C)** for 6 h, and leaves were collected and then stained with NBT. Superoxide accumulation was shown as blue precipitates. **(F)** The accumulation of hydrogen peroxide induced by FB_1. Plants were treated as described in **(C)** for 6 h, and leaves were collected and then stained with DAB. Hydrogen peroxide accumulation was shown as dark brown precipitates. Bar, 2 mm (**A** and **B**).

Molecular cloning of the FBR11 gene

Genetic analysis indicated that the *fbr11-1* mutant genome contained a single T-DNA insertion (kanamycin resistant:sensitive = 246:85, χ^2=0.04933; p<0.05). When transferred from an FB_1 medium to a kanamycin medium, all 147 *fbr11-1* seedlings showed resistance to the antibiotic, suggesting that the T-DNA was tightly co-segregated with the mutation. To identify the *FBR11* candidate gene, TAIL-PCR [37] was used to isolate the genomic sequences flanking to the Left Border (LB) of the T-DNA. DNA sequencing analysis indicated that the LB was inserted in At4g36480 approximately 260 base pairs downstream from the stop codon (Figure 3A). PCR analysis indicated that the putative At4g36480 open reading frame (ORF) remained intact. However, a real-time quantative reverse transcription

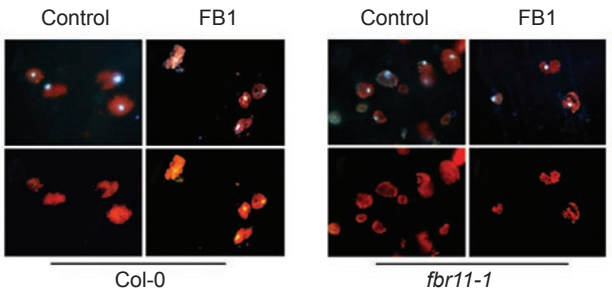

Figure 2 Nuclear DNA fragmentation in WT and *fbr11-1* protoplast induced by FB_1. Protoplasts prepared from WT or *fbr11-1* leaves were treated with methanol (0.005%; control) or 50 nM FB_1 for 10 h. DNA molecules were then stained with Hoechst 33342 (blue signals in the upper panels), and 3′-OH groups were stained by the TUNEL method (orange signals in the lower panels). The experiment was repeated for three times (n>100 in each set of samples).

(RT)-PCR analysis revealed that the *FBR11* expression was substantially reduced in *fbr11-1* (Figure 3B).

To verify the identity of *FBR11*, we carried out a molecular complementation experiment. A 4.7-kilo base pairs (Kb) WT genomic DNA fragment, which encompassed the promoter region, the coding sequence and a portion of the 3′UTR of At4g36480, was cloned into a binary vector pER8 [39]. The resulting construct was then transformed into *fbr11-1* plants. The At4g36480 transgene was able to fully restore the sensitivity of *fbr11-1* to FB_1, including the growth arrest phenotype (Figure 3C), the cell death phenotype as well as the accumulation of ROIs (Figure 3D). These results indicate that At4g36480 represents the *FBR11* gene.

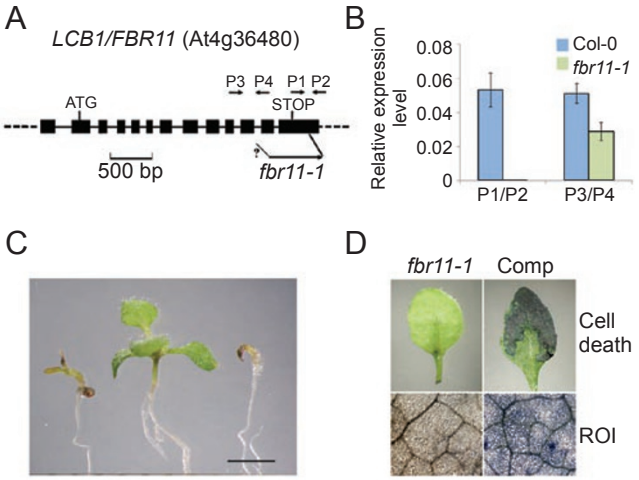

Figure 3 Molecular characterization of *FBR11*. **(A)** Schematic representation of the *FBR11* gene. Exons and introns are represented by filled boxes and lines, respectively. Untranscribed and untranslated regions (UTR) are indicated as dashed lines. The insertion site and the orientation of the T-DNA insertion (arrow indicates the orientation of the left border or LB) in the *fbr11-1* genome are shown. Insertion site for the right border (RB) is unclear (indicated by a question mark). UTR sequences were derived from the cDNA sequence (GenBank accession AY120759). **(B)** Quantative real-time RT-PCR analysis of *FBR11* expression in WT and *fbr11-1*. RNA prepared from three-week-old seedlings germinated and grown on MS medium was used for the synthesis of the first strand cDNA using oligo-dT as a primer. PCR was carried out using primer pairs as shown in panel A (P1 through P4; the insertion site of LB was between P1 and P2). Relative expression levels were normalized to that of *Actin7*. Mean values of two independent experiments were shown in the graph. Bars represent standard errors. **(C)** Molecular complementation of the *fbr11-1* phenotype. An *FBR11* WT genomic DNA fragment (including the *FBR11* promoter sequence) was cloned into a binary vector, and the resulting construct was transformed into *fbr11-1*. T2 transgenic plants were grown on MS medium supplemented with 1 μM FB_1 for 2 weeks. From left to right in each panel: WT, *fbr11-1*, and *fbr11-1* carrying an *FBR11* transgene. Fourteen independent transgenic lines were tested, and similar results were obtained. Bar, 2 mm. **(D)** Rescue of the cell death and superoxide generation phenotypes in *fbr11-1*. T2 transgenic plants as described in panel C were treated with 0.02% methanol (left) or 2 μM FB_1 (right) by spraying. Leaves were collected for assays of cell death (24 h) and superoxide accumulation (6 h) as described in Figure 1. Three independent transgenic lines were tested and similar results were obtained. Comp: complemented transgenic plants.

FBR11 encodes an LCB1 subunit of serine palmitoyltransferase

FBR11 is a single copy gene in the *Arabidopsis* genome. A full-length *FBR11* cDNA clone was identified from the database (accession number: AY120759). Comparison of the cDNA and genomic sequences revealed that *FBR11* contains 12 introns (Figure 3A). An ORF within the *FBR11* gene encodes a polypeptide of 482 amino acid residues, with a predicted molecular mass of 53.14 KDa and a pI of 7.23. Sequence comparison revealed that *FBR11* encodes a putative LCB1 subunit of SPT, catalyzing the formation of 3-ketosphinganine during sphingolipid *de novo* synthesis (Figure 4). During the course of this study, Chen *et al*. [41] reported the characterization of *LCB1/FBR11*. Coexpression of *LCB1/FBR11* and *LCB2* cDNA was able to complement the long-chain base auxotrophy of *S. cerevisiae lcb1*Δ and *lcb2*Δ single and double mutants, indicating that both LCB1 and LCB2 are functional subunits of SPT. Moreover, *lcb1-1*, a stronger mutant allele than *fbr11-1*, was suggested to cause abnormal embryo development [41].

Measurement of sphingolipids in Arabidopsis

The fact that *FBR11* encodes an LCB1 subunit of SPT prompted us to ask whether sphingolipid metabolism has been altered by the *fbr11* mutation. To address this question, we compared levels of several species of sphingolipids in *fbr11-1* with those of WT plants. Total lipids were extracted from 3-week-old seedlings, and sphingolipids were then subjected to tandem Mass Spectrum (MS/MS) analysis using authentic standards. In WT plants, among the assayed sphingolipids, the most predominant sphingoid bases are phyto-sph and phytosphingosine-1-phosphate (phyto-S1P), followed by dh-sph and dihydrosphingosine-1-phosphate (dh-S1P) (Table 1). Similarly, the main ceramides also appeared to be the phyto- and dihydro-types. Notably, whereas phyto-C16-, phyto-C24- and phyto-C24:1-ceramides were the major species in *Arabidopsis*, phyto-C14, dhC16-, phyto-C20- and C24:1-ceramides as well as all C18-derivatives appeared to be less abundant (Table 1). We note that our measurements of dh-sph and phyto-sph levels were comparable with those of a previous study on tomato, duckweed and tobacco calli [17]. Under our assay

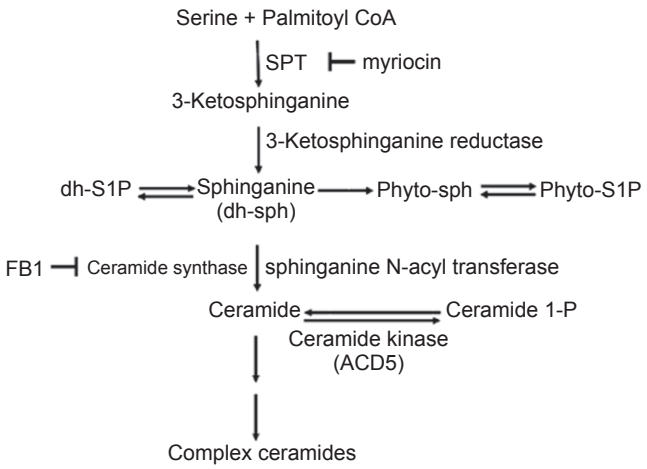

Figure 4 A proposed pathway of plant sphingolipid *de novo* synthesis. Myriocin and FB_1 are competitive inhibitors of SPT and ceramide synthase, respectively (Modified from [13]).

conditions, most non-phyto/dihydro-type sphingoid bases and ceramides were present only in trace amounts (Table 1). S1P, for example, was found to be approximately 18-fold less abundant than phyto-S1P. Again, in agreement with an earlier report on *Commelina communis*, in which S1P was estimated at 5-46 pg per g dry weight [24], the compound was approximately 10-40 pg per g dry weight in our assays.

Sphingolipid metabolism in fbr11-1

To monitor possible effects of the *fbr11-1* mutation on ceramide metabolism, we compared several sphingolipid species in the mutant with those found in WT plants. It appeared that the mutation did not cause substantial changes among the tested sphingolipids (Table 1). We then reasoned

Table 1 Measurement of sphingolipids in wild type and *fbr11-1* mutant plants

	Col-0	Col-0/FB_1	*fbr11-1*	*fbr11-1*/FB_1
dh-sph	14.52±1.62	1122.01±203.79	14.82±5.01	350.34±75.86
sph	1.89±0.36	1.54±0.68	0.75±0.47	1.92±0.11
Phyto-sph	2605.40±279.44	31951.43±2261.79	2012.01±166.16	12828.69±1123.90
S1P	2.16±0.32	1.38±0.01	1.49±0.48	1.89±0.85
Phyto-S1P	39.62±3.41	6421.92±837.25	31.76±15.47	1671.37±577.86
dh-S1P	6.23±0.71	898.23±257.18	5.41±1.13	208.27±133.95
Phyto-C14-Cer	13.01±3.90	11.48±1.08	11.59±3.05	11.84±0.17
dh-C16-Cer	37.67±1.39	35.70±12.42	41.64±5.02	35.15±2.70
Phyto-C16-Cer	102.93±5.07	154.19±46.68	136.62±63.75	80.99±23.83
C18-Cer	9.99±2.61	3.79±0.59	7.47±0.96	5.39±2.32
Phyto-C18-Cer	7.13±0.20	8.76±1.88	13.24±3.97	11.35±3.11
Phyto-C18:1-Cer	7.82±0.44	6.54±1.67	8.15±3.66	7.38±0.91
Phyto-C20-Cer	15.72±5.08	14.86±5.65	14.17±2.65	18.55±3.35
C24:1-Cer	13.11±3.99	25.52±14.24	15.78±3.78	23.46±10.16
Phyto-C24:1-Cer	592.66±51.68	557.11±131.92	590.33±52.95	499.04±33.25
Phyto-C24-Cer	1480.98±0.04	1558.82±206.96	1567.24±70.62	1466.35±23.12

1. Three-week-old seedlings were treated with 5 μM FB_1 for 1, 3, 6, 12 and 24 h by spraying (2 ml per 90-mm Petri dish), respectively. Samples were harvested and immediately frozen in liquid nitrogen. Sphingolipids were prepared and analyzed as described in Materials and Methods.

2. Data presented are obtained from samples treated with 5 μM FB_1 for 6 h, and are mean values obtained from three independent experiments. Standard deviations are also shown. Shorter (3 h) or longer treatment (12 and 24 h) did not significantly affect the sphingolipid levels under the assay conditions (data not shown). When treated for 1 h, less but substantial alterations were observed in several major species, including dh-sph (FB_1-treated-Col-0 and *fbr11-1* were 5.6- and 4.5-fold higher than that of the untreated samples, respectively), phyto-sph (13.7 and 11.0), phyto-S1P (22.8 and 17.9), dh-S1P (6.8 and 4.0), phyto-C16-Cer (4.4 and 3.3), phyto-C24:1-Cer (3.0 and 2.3) and phyto-C24-Cer (3.7 and 3.1).

3. All concentrations are expressed as pmol per g fresh weight.

4. Several analyzed ceramides (C14-, C16-, C18-, C18:1-, C20- and C24-Cer), which are under the detection limit or close to the background level, are not shown in the Table.

5. Owing to the unavailability of authentic standards, several major species, including the most abundant free LCB 8-sphingenine, 4,8-sphingadienine, and 4-hydroxy-8-sphingenine, were not measured.

6. Phyto-C14- and Phyto-C20-ceramides, for which no authentic standards are available, were quantified using the calibration curve of Phyto-C18-ceramide.

that because *fbr11-1* was resistant to FB_1, a comparison of sphingolipids between the mutant and WT plants treated with the apoptosis-inducing compound might provide clues concerning the molecular mechanism of plant PCD. In both WT and *fbr11-1* plants, FB_1-treatment caused a massive increase of several major sphingoid bases (Table 1). Substantially altered levels in several species could be observed upon treatment with FB_1 for 1 h (see Note 2 of Table 1). In WT plants, the most significant alterations were found in several sphingoid bases, including dh-sph (77-fold), phyto-sph (12-fold), phyto-S1P (162-fold) and dhS1P (144-fold). Under the same conditions, however, the FB_1-resistant *fbr11-1* mutant plants accumulated less of these sphingoid bases (23-, 6-, 53-, and 39-fold, respectively; Table 1). In contrast to those of free sphingoid bases, levels of ceramides were marginally altered in all cases, suggesting that FB_1-induced PCD is likely related to the accumulation of sphingoid bases or an altered balance among these compounds. Moreover, compared to that of WT, the substantially altered sphingoid base levels in the mutant treated by FB_1 suggest a role of *FBR11* in sphingolipid metabolism.

Activation of PCD in Arabidopsis by free sphingoid bases

Altered sphingolipid levels in WT and *fbr11-1* treated with FB_1 suggested that sphingoid bases may play an important role in regulating PCD in *Arabidopsis*. To ask if these compounds are capable of triggering PCD in *Arabidopsis*, we treated WT plants with different sphingoid bases, followed by monitoring ROI generation and cell death in detached leaves. As shown in Figure 5, while dh-sph, phyto-sph and sph were able to induce ROI production and cell death, their phosphorylated derivatives, dh-S1P, phyto-S1P and S1P, did not have the PCD-inducing effect under the assay conditions. Moreover, the PCD-inducing effect of dh-sph, phyto-sph and sph was dose-dependent in both WT and *fbr11-1* leaves (Figure 5B-5D). We reproducibly observed that dh-sph was less potent than phyto-sph, consistent with a previous finding that phyto-sph displays greater phototoxicity than dh-sph [42]. The fact that WT and *fbr11-1* responded to exogenous dh-sph, phyto-sph and sph in an indistinguishable manner suggested that the perception and subsequent amplification of a death signal were not affected by the mutation. We conclude from these data that free sphingoid bases, but not their phosphorylated derivatives, can trigger PCD in *Arabidopsis*, presumably by regulating ROI production.

Inhibition of dh-sph-induced ROI generation and PCD by dh-S1P

The above data indicated that the phosphorylated forms of sphingoid bases are incapable of inducing PCD in plant cells. Moreover, among the analyzed free sphingoid bases, dh-sph is the only compound that displayed an altered level in both FB_1- and paraquat-treated plants (Table 1 and data not shown). Therefore, alterations of dh-sph concentration and/or the ratio between this sphingoid base and its phosphorylated form may play a role in the regulation of PCD in *Arabidopsis*. To test this hypothesis, we treated WT seedlings with 2 μM dh-sph combined with its phosphorylated form dh-S1P at different concentrations. Figure 6A shows that ROI generation and cell death induced by dh-sph were efficiently blocked by dh-S1P in a dose-dependent manner.

Whereas this result suggested an anti-apoptotic role of dh-S1P, an alternative possibility could be that ROI generation and cell death might also be regulated by the ratio of a free sphingoid base and its phosphorylated form. To distinguish these two possibilities, we then tested if dh-S1P also had a protective effect against ROI generation and cell death induced by other treatments. When treated by phyto-sph or paraquat, neither ROI production nor cell death could be reduced by dh-S1P (Figure 6B). These observations suggest that the balance between dh-sph and its phosphorylated form dh-S1P plays an important role in the control of ROI-modulated PCD in *Arabidopsis*.

Discussion

In this study, we have presented genetic, biochemical and molecular evidence showing that *FBR11* encodes an LCB1 of SPT, and sphingoid bases are directly involved in the regulation of PCD in plant cells, presumably through controlling ROI production. First, FB_1 causes a variety of cellular and molecular alterations characteristics of apoptotic cells, including the accumulation of ROIs and fragmentation of nuclear DNA. Second, mutation in the *FBR11* gene renders the mutant resistant to FB_1, and the anti-apoptotic phenotype of the mutation is correlated with the cellular and molecular alterations commonly associated with plant PCD. These observations suggest that *FBR11* is involved in the regulation of the PCD signaling pathway. Third, molecular and genetic analyses indicate that *FBR11* encodes an LCB1. Notably, alterations of the sphingolipid level (1 h after FB_1 treatment) are prior to ROI production (3-6 h) and cell death (22-24 h). These observations suggest that an altered sphingolipid level may lead to ROI production, thereby causing cell death. Finally, we showed that whereas dh-sph, phyto-sph and sph were capable of efficiently inducing ROI generation and cell death, dh-S1P specifically blocked the apoptotic effect induced by dh-sph, suggesting that free sphingoid bases and their phosphorylated derivatives play an important role in regulating ROI

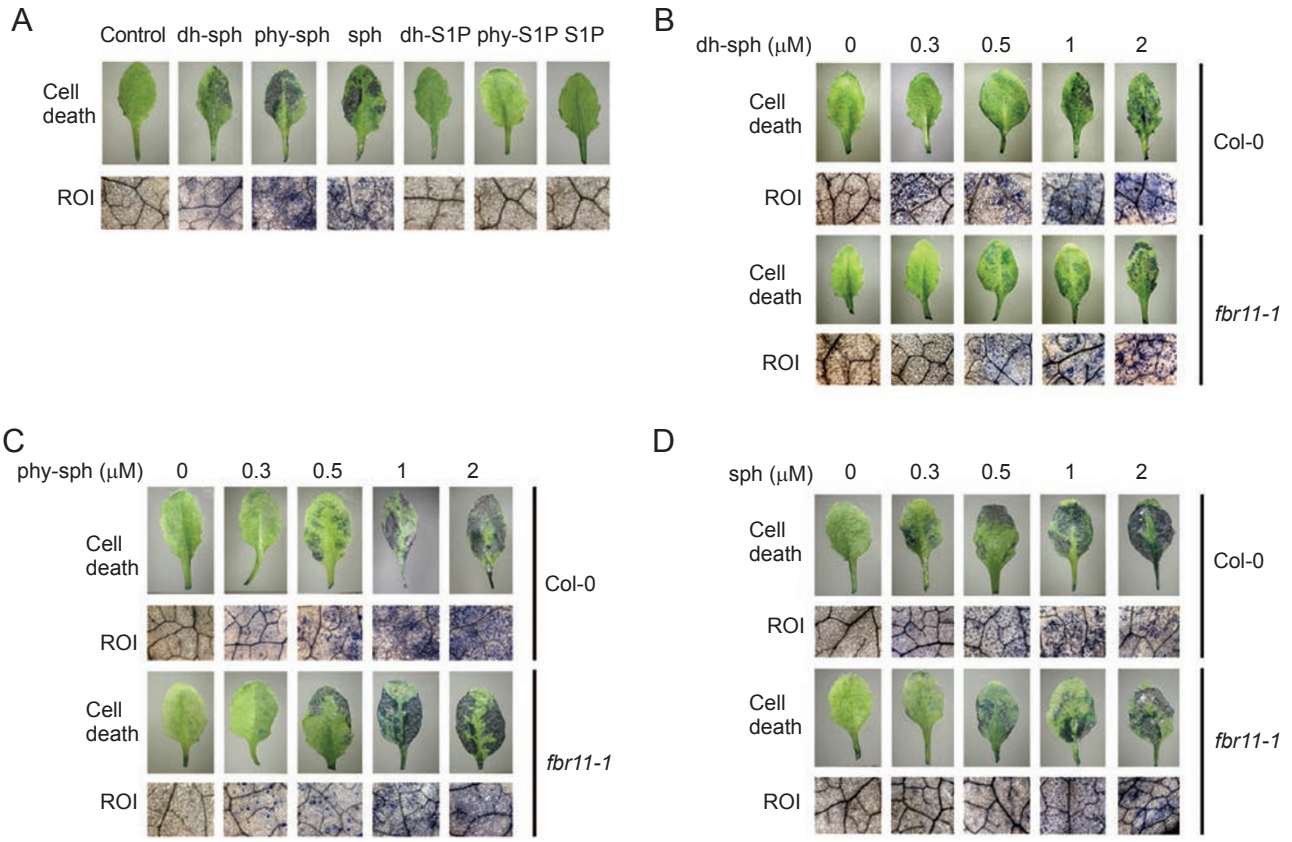

Figure 5 ROI generation and cell death induced by free sphingoid bases. **(A)** PCD-inducing effects of free sphingoid bases and their phosphorylated derivatives. WT Col-0 plants were treated with 1 μM of each compound as indicated on the top of the panel for 24 h (top row; cell death) or 6 h (bottom row; ROIs), respectively. See Figure 1 for other technical details. **(B-D)** Dose-dependent effects of free sphingoid bases on the induction of cell death and ROI production. WT Col-0 and *fbr11-1* plants were treated with different concentrations of dh-sph **(B)**, phyto-sph **(C)** or sph **(D)** as described in panel **(A)**. The concentrations of the free sphingoid bases in the experiments are indicated on the top of each panel. See Figure 1 for other technical details.

generation, thereby determining the cell fate.

FBR11 encodes an LCB1 of SPT, which consists of two subunits, LCB1 and LCB2. It has been suggested that LCB2 acts as the enzymatically active center, and LCB1 appears to stabilize the heterodimer [14]. The *lcb1* mutations caused a substantially reduced level of the LCB2 protein in both a Chinese hamster ovary cell mutant line [43] and yeast cells [44], thus leading to lethality in both cases. Similarly, the *lcb1-1* mutation causes an embryo-lethal phenotype, indicating an essential role of *FBR11* in plant growth and development [41]. However, a striking phenotype of *fbr11-1* appears to be its resistance to FB_1. As competitive inhibitors of ceramide synthase, FB_1 and AAL toxin both caused markedly increased levels of several sphingolipid species [15, 17, 45]. This might account for the cell death phenotype in a number of cases [16-19, 45, 46]. Ceramide synthase was proposed to be a multi-subunit complex, of which members of the yeast longevity assurance gene (*LAG1*) family, including the tomato *ASC1* gene [47], are the only components identified thus far [12, 48]. Whereas the dominant *ASC1* allele confers FB_1- and AAL toxin-resistance to tomato [15, 49], overexpression of the mammalian *LAG1* homologs *UOG1* [50], *TRH1* and *TRH4* [51] renders 293T cells resistant to FB_1. Conversely, the recessive *asc1* isogenic line is sensitive to the toxins [15, 49]. However, the toxin-susceptibility of *asc1*, which appears to be correlated to an elevated level of dh-sph and phyto-sph [17, 45], can be partially relieved by myriocin [45]. Similarly, myriocin is also able to enhance the resistance to FB_1 in *Arabidopsis* (our unpublished data). Consistent with these observations, the *fbr11-1* mutation, which presumably causes a reduced SPT activity, also leads to resistance to FB_1. Thus, it appears that a decreased SPT activity, either by mutations or an enzymatic inhibitor of

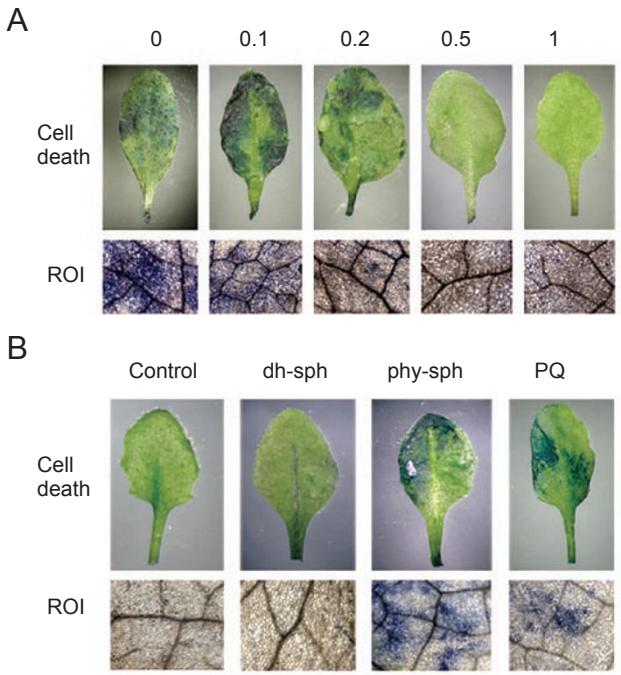

Figure 6 Dh-S1P specifically blocks ROI generation and cell death induced by dh-sph. **(A)** Dh-S1P blocks ROI generation and cell death induced by dh-sph. WT Col-0 plants were treated with a solution containing 2 μM dh-sph and various concentrations of dh-S1P as indicated on the top of the panel for 24 h (top row) or 6 h (bottom row), respectively. See Figure 1 for other technical details. **(B)** Dh-S1P specifically inhibits ROI generation and cell death induced by dh-sph, but not by phyto-sph or paraquat. WT Col-0 plants were treated with a solution containing 1 μM dh-S1P along with 1 μM dh-sph, 1 μM phyto-sph or 3 μM paraquat as indicated on the top of the panel for 24 h (top row) or 6 h (bottom row), respectively. See Figure 1 for other technical details.

SPT, can partially compensate for a dysfunctional ceramide synthase, thereby reducing or preventing the generation of the death signal(s) in plant cells.

Because an impaired ceramide synthase causes PCD, the death signal(s) are likely the substrates of the enzyme. The currently known substrates of the enzyme include dh-sph and sph [10, 12, 13], which accumulate to substantially high levels upon treatment with FB_1 or AAL toxin in a variety of plant species [17, 21, 45] (see also Table 1) as well as several mammalian cell lines [14, 52]. The observation that FB_1 causes massively increased sphingoid bases suggests that these compounds are key signal molecules that control plant PCD. In the FB_1-treated plants, the phosphorylated sphingoid bases phyto-S1P and dh-S1P increase at a significantly higher level compared to their free bases (Table 1). However, in contrast to that observed in *Saccharomyces cerevisiae* [53], these phosphorylated sphingoid bases are incapable of activating PCD in *Arabidopsis*. These observations suggest that different mechanisms may operate in yeast and plants. Instead, several free sphingoid bases are able to efficiently and specifically induce ROI generation and cell death. Therefore, the FB_1-resistant phenotype of *fbr11-1* is presumably due to a reduced level of free sphingoid bases (see also below).

Upon FB_1 treatment, levels of several free sphingoid bases increased remarkably, although a lower level of these compounds was found in *fbr11-1*. These results suggest that an elevated level of free sphingoid bases alone is not sufficient to account for the PCD-inducing effect of the toxin. The observation that dh-S1P specifically blocks ROI generation and cell death induced by dh-sph, but not by phyto-sph and paraquat, implies that a proper balance between a free sphingoid base and its phosphorylated form is also important for the control of plant PCD. Consistent with these findings, C2-ceramide induces, but its phosphorylated form partially blocks, PCD in *Arabidopsis* protoplasts [23]. Similar observations were also made in animal cells, in which the balance between sph and S1P, but rather than their absolute concentrations, was thought to determine the cell fate and other physiological consequences [54]. It however should be pointed out that both the increased levels of free sphingoid bases and an altered balance between a free sphingoid base and its phosphorylated form may play a role in the regulation of plant PCD. Currently we are unable to clearly distinguish these two possibilities or determine which factor plays a more dominant role.

Sphingolipid-regulated PCD in plant cells has long been appreciated, but the biochemical mechanism of the regulation remains largely unclear. We show that ROI generation is prior to the onset of cell death but after the sphingolipid alterations in FB_1-treated WT plants. Conversely, no ROI accumulation was observed in the FB_1-resistant *fbr11-1* mutant plants. Moreover, when treated with dh-sph, phyto-sph and sph, ROI generation also appears to be required for cell death. Lastly, the anti-apoptotic effect of dh-S1P is also correlated with its inhibition of ROI generation. These observations suggest that the sphingolipid-mediated cell death is coupled with the generation of ROIs, which, in turn, may activate a downstream PCD pathway. Among the currently known components involved in the ROI-mediated signaling, the structurally related zinc-finger proteins LSD1 and LOL1 presumably act to monitor the cellular ROI levels [32, 55, 56], whereas the serine/threonine protein kinase OXI1 appears to link an oxidative burst signal with diverse downstream responses [57]. Moreover, overexpression of the *Arabidopsis* Bax Inhibitor-1 renders the transgenic plants insensitive to ROIs induced by a number of stimuli [58]. Although possible interactions among these signal-

ing components remain unknown, it will be of interest to examine the sphingolipid-regulated PCD with respect to these genetic loci. Despite the critical regulatory role of sphingolipids in the control of ROI generation and PCD as revealed by this study, the biochemical mechanism of this regulation unfortunately remains to be elucidated. Moreover, identification of the cellular targets of sphingolipids will be a key to fully understanding the complicated regulatory machinery that controls PCD in plant cells, and will likely shed light on the mechanisms of other sphingolipid-regulated signaling activities in plant cells.

Acknowledgments

We would like to thank the Arabidopsis Biological Resources Center (Ohio State University, USA) for providing seeds and Dr Teresa Dunn (Uniformed Services University of the Health Sciences, USA) for providing yeast strains. We are grateful to Drs Weicai Yang, Yongbiao Xue (Institute of Genetics and Developmental Biology, Chinese Academy of Sciences) and De Ye (China Agriculture University) for critical reading of the manuscript. This work was supported by grants from the National Natural Science Foundation of China (30330360, 30125025 and 30221002) and the Chinese Academy of Sciences to Jianru Zuo.

References

1 Pennell RI, Lamb C. Programmed cell death in plants. Plant Cell 1997; **9**:1157-1168.
2 Lam E, Kato N, Lawton M. Programmed cell death, mitochondria and the plant hypersensitive response. Nature 2001; **411**:848-853.
3 Morel JB, Dangl JL. The hypersensitive response and the induction of cell death in plants. Cell Death Differ 1997; **4**:671-683.
4 Dangl JL, Jones JD. Plant pathogens and integrated defence responses to infection. Nature 2001; **411**:826-833.
5 Lorrain S, Vailleau F, Balague C, Roby D. Lesion mimic mutants: keys for deciphering cell death and defense pathways in plants? Trends Plant Sci 2003; **8**:263-271.
6 Parker JE. Plant recognition of microbial patterns. Trends Plant Sci 2003; **8**:245-247.
7 Feys BJ, Parker JE. Interplay of signaling pathways in plant disease resistance. Trends Genet 2000; **16**:449-455.
8 Richberg MH, Aviv DH, Dangl JL. Dead cells do tell tales. Curr Opin Plant Biol 1998; **1**:480-485.
9 Richael C, Gilchrist D. The hypersensitive response: A case of hold or fold? Physiol Mol Plant Pathol 1999; **55**:5-12.
10 Sperling P, Heinz E. Plant sphingolipids: structural diversity, biosynthesis, first genes and functions. Biochimica et Biophysica Acta 2003; **1632**:1-15.
11 Worrall D, Ng CK, Hetherington AM. Sphingolipids, new players in plant signaling. Trends Plant Sci 2003; **8**:317-320.
12 Spassieva SD, Hille J. Plant sphingolipids today - are they still enigmatic? Plant biol 2003; **5**:125-136.
13 Lynch DV, Dunn TM. An introduction to plant sphingolipids and a review of recent advances in understanding their metabolism and function. New Phytol 2004; **161**:677-702.
14 Hanada K. Serine palmitoyltransferase, a key enzyme of sphingolipid metabolism. Biochim Biophys Acta 2003; **1632**:16-30.
15 Wang E, Norred WP, Bacon CW, Riley RT, Merrill AHJ. Inhibition of sphingolipid biosynthesis by fumonisins. Implications for diseases associated with *Fusarium moniliforme.* J Biol Chem 1991; **266**:14486-14490.
16 Gilchrist DG, Wang H, Bostock RM. Sphingosine-related mycotoxins in plant and animal diseases. Can J Bot 1994; **73**: S459-S467.
17 Abbas HK, Tanaka T, Duke SO, *et al*. Fumonisin- and AAL-toxin-induced disruption of sphingolipid metabolism with accumulation of free sphingoid bases. Plant Physiol 1994; **106**:1085-1093.
18 Wang H, Li J, Bostock RM, Gilchrist DG. Apoptosis: A functional paradigm for programmed plant cell death induced by a host-selective phytotoxin and invoked during development. Plant Cell 1996; **8**:375-391.
19 Asai T, Stone JM, Heard JE, *et al*. Fumonisin B1-induced cell death in *Arabidopsis* protoplasts requires jasmonate-, ethylene-, and salicylate-dependent signaling pathways. Plant Cell 2000; **12**:1823-1835.
20 Stone JM, Heard JE, Asai T, Ausubel FM. Simulation of fungal-mediated cell death by fumonisin B1 and selection of *fumonisin B1-resistant* (*fbr*) *Arabidopsis* mutants. Plant Cell 2000; **12**:1811-1822.
21 Brodersen P, Petersen M, Pike HM, *et al*. Knockout of *Arabidopsis ACCELERATED-CELL-DEATH11* encoding a sphingosine transfer protein causes activation of programmed cell death and defense. Genes Dev 2002; **16**:490-502.
22 Greenberg JT, Silverman FP, Liang H. Uncoupling salicylic acid-dependent cell death and defense-related responses from disease resistance in the *Arabidopsis* mutant *acd5*. Genetics 2000; **156**:341-350.
23 Liang H, Yao N, Song JT, *et al*. Ceramides modulate programmed cell death in plants. Genes Dev 2003; **17**:2636-2641.
24 Ng CK, Carr K, McAinsh MR, Powell B, Hetherington AM. Drought-induced guard cell signal transduction involves sphingosine-1-phosphate. Nature 2001; **410**:596-599.
25 Coursol S, Fan LM, Le Stunff H, *et al*. Sphingolipid signalling in *Arabidopsis* guard cells involves heterotrimeric G proteins. Nature 2003; **423**:651-654.
26 Pandey S, Assmann SM. The *Arabidopsis* putative G protein-coupled receptor GCR1 interacts with the G protein a subunit GPA1 and regulates abscisic acid signaling. Plant Cell 2004; **16**:1616-1632.
27 Murashige T, Skoog F. A revised medium for rapid growth and bioassays with tobacco tissue culture. Physiol Plant 1962; **15**:473-497.
28 Zuo J, Niu QW, Frugis G, Chua N-H. The *WUSCHEL* gene promotes vegetative-to-embryonic transition in *Arabidopsis*. Plant J 2002; **30**:349-359.
29 Bechtold N, Ellis J, Pelletier G. *In planta Agrobacterium*-mediated gene transfer by infiltration of adult *Arabidopsis thaliana* plants. C R Acad Sci Ser III Sci Vie 1993; **316**:1194-1199.
30 Zhang J, Xu J, Kong Y, *et al*. Generation of chemical-inducible activation tagging T-DNA insertion lines of *Arabidopsis thaliana.* Yi Chuan Xue Bao 2005; **32**:1082-1088.

31 Feng H, Chen Q, Feng J, *et al*. Functional Characterization of the *Arabidopsis* Eukaryotic Translation Initiation Factor 5A-2 That Plays a Crucial Role in Plant Growth and Development by Regulating Cell Division, Cell Growth, and Cell Death. Plant Physiol 2007; **144**:1531-1545.
32 Jabs T, Dietrich RA, Dangl JL. Initiation of runaway cell death in an *Arabidopsis* mutant by extracellular superoxide. Science 1996; **273**:1853-1856.
33 Kim M, Ahn JW, Jin UH, *et al*. Activation of the programmed cell death pathway by inhibition of proteasome function in plants. J Biol Chem 2003; **278**:19406-19415.
34 Rusterucci C, Aviv DH, Holt III BF, Dangl JL, Parker J. The disease resistance signaling components *EDS1* and *PAD4* are essential regulators of the cell death pathway controlled by *LSD1* in *Arabidopsis*. Plant Cell 2001; **13**:2211-2224.
35 Bielawski J, Szulc ZM, Hannun YA, Bielawska A. Simultaneous quantitative analysis of bioactive sphingolipids by high-performance liquid chromatography-tandem mass spectrometry. Methods 2006; **39**:82-91.
36 Sambrook J, Russell DW. Molecular cloning: A Laboratory Manual. Cold Spring Harbor Laboratory Press: Cold Spring Harbor, NY 2001.
37 Liu YG, Mitsukawa N, Oosumi T, Whittier RF. Efficient isolation and mapping of *Arabidopsis thaliana* T-DNA insert junctions by thermal asymmetric interlaced PCR. Plant J 1995; **8**:457-463.
38 Sun J, Niu Q-W, Tarkowski P, *et al*. The *Arabidopsis AtIPT8/PGA22* gene encodes an isopentenyl transferase that is involved in *de novo* cytokinin biosynthesis. Plant Physiol 2003; **131**:167-176.
39 Zuo J, Niu QW, Chua NH. An estrogen receptor-based transactivator XVE mediates highly inducible gene expression in transgenic plants. Plant J 2000; **24**:265-273.
40 Dong H, Deng Y, Mu J, *et al*. The *Arabidopsis* Spontaneous Cell Death1 gene, encoding a [zeta]-carotene desaturase essential for carotenoid biosynthesis, is involved in chloroplast development, photoprotection and retrograde signalling. Cell Res 2007; **17**:458-470.
41 Chen M, Han G, Dietrich CR, Dunn TM, Cahoon EB. The Essential Nature of Sphingolipids in Plants as Revealed by the Functional Identification and Characterization of the *Arabidopsis* LCB1 Subunit of Serine Palmitoyltransferase. Plant Cell 2006; **18**:3576-3593.
42 Tanaka T, Abbas HK, Duke S. Structure-dependent phytotoxicity of fumonisins and related compounds in duckweed bioassay. Phytochemistry 1993; **33**:779-785.
43 Yasuda S, Nishijima M, Hanada K. Localization, topology, and function of the LCB1 subunit of serine palmitoyltransferase in mammalian cells. J Biol Chem 2003; **278**:4176-4183.
44 Gable K, Slife H, Bacikova D, Monaghan E, Dunn TM. Tsc3p is an 80-amino acid protein associated with serine palmitoyltransferase and required for optimal enzyme activity. J Biol Chem 2000; **275**:7597-7603.
45 Spassieva SD, Markham JE, Hille J. The plant disease resistance gene *Asc-1* prevents disruption of sphingolipid metabolism during AAL-toxin-induced programmed cell death. Plant J 2002; **32**:561-572.
46 Gilchrist DG. Programmed cell death in plant disease: The purpose and promise of cellular suicide. Annu Rev Phytopathol 1998; **36**:393-414.
47 Brandwagt BF, Mesbah LA, Takken FLW, *et al*. A longevity assurance gene homolog of tomato mediates resistance to *Alternaria alternata f. sp. lycopersici* toxins and fumonisin B1. Proc Nat Acad Sci USA 2000; **97**:4961-4966.
48 Dunn TM, Lynch DV, Michaelson LV, Napier JA. A post-genomic approach to understanding sphingolipid metabolism in *Arabidopsis thaliana.* Annals of Botany 2004; **93**:483-497.
49 Clouse SD, Gilchrist DG. Interaction of the *asc* locus in F8 paired lines of tomato with *Alternaria alternata f.sp. lycopersici* AAL-toxin. Phytopathology 1987; **77**:80-82.
50 Venkataraman K, Riebeling C, Bodennec J, *et al*. Upstream of growth and differentiation factor 1 (uog1), a mammalian homolog of the yeast *Longevity Assurance Gene 1* (*LAG1*), regulates N-stearoyl-sphinganine (C18-(dihydro)ceramide) synthesis in a fumonisin B1-independent manner in mammalian cells. J Biol Chem 2002; **277**:35642-35649.
51 Riebeling C, Allegood JC, Wang E, Merrill AH, Jr, Futerman AH. Two mammalian longevity assurance gene (LAG1) family members, trh1 and trh4, regulate dihydroceramide synthesis using different fatty Acyl-CoA donors. J Biol Chem 2003; **278**:43452-43459.
52 Desai K, Sullards MC, Allegood J, *et al*. Fumonisins and fumonisin analogs as inhibitors of ceramide synthase and inducers of apoptosis. Biochim Biophys Acta 2002; **1585**:188-192.
53 Kim S, Fyrst H, Saba J. Accumulation of phosphorylated sphingoid long chain bases results in cell growth inhibition in *Saccharomyces cerevisiae.* Genetics 2000; **156**:1519-1529.
54 Spiegel S, Milstien S. Sphingosine-1-phosphate: an enigmatic signalling lipid. Nat Rev Mol Cell Biol 2003; **4**:397-407.
55 Dietrich RA, Richberg MH, Schmidt R, Dean C, Dangl JL. A novel zinc finger protein is encoded by the *Arabidopsis LSD1* gene and functions as a negative regulator of plant cell death. Cell 1997; **88**:685-694.
56 Epple P, Mack AA, Morris VRF, Dangl JL. Antagonistic control of oxidative stress-induced cell death in *Arabidopsis* by two related, plant-specific zinc finger proteins. Proc Nat Acad Sci USA 2003; **100**:6831-6836.
57 Rentel MC, Lecourieux D, Ouaked F, *et al*. OXI1 kinase is necessary for oxidative burst-mediated signalling in *Arabidopsis.* Nature 2004; **427**:858-861.
58 Kawai-Yamada M, Ohori Y, Uchimiya H. Dissection of *Arabidopsis* Bax inhibitor-1 suppressing Bax-, hydrogen peroxide-, and salicylic acid-induced cell death. Plant Cell 2004; **16**:21-32.